Pages: 1-16 / Vol. 18 / Issue 2 / Summer - Fall 2025

Journal of Aerospace Science and Technology

Journal Homepage: https://jast.ias.ir

Original Research Article

Effects of Syngas H2/CO Composition and Turbulent Intensity on the Bluff-Body Premixed Combustion Characteristics

Negar Nabatian[1]* and Vahid Nourmohammadi [2]

Faculty of Mechanical and Energy Engineering, Shahid Beheshti University, Tehran, Iran

ARTICLE INFO

Received: 29 August 2024
Revised: 22 January 2025
Accepted: 25 January 2025
Available online: 07 May 2025

KEYWORDS:

Syngas
Premixed flames
Bluff body
Chemical kinetics
Lean blowout limit

ABSTRACT

The effects of hydrogen content variation in H2/CO composition with different turbulent intensities were numerically investigated. The GRI3.0 reduced mechanism, including 15 species and 46 subreactions with scale-adaptive simulation (SAS) turbulence model and eddy-dissipation concept (EDC) turbulence-chemistry interaction, was utilized in FLUENT. In lean combustion, by increasing hydrogen content, the production of "OH" radicals is increased, and they consume "CO" drastically, leading to a high "CO" consumption rate. In rich combustion, as hydrogen concentration rises, "OH" and O radicals tend to react with hydrogen instead of "CO" due to hydrogen's higher reactivity, decreasing "CO" the consumption rate. With hydrogen concentration enhancement, the amount of vapor products rises, causing the products' heat capacity to increase. Then, the produced combustion heat, flame temperature, and produced "NO" gases are decreased. The maximum flame temperature "NO" occurs at the equivalence ratios of 1.1 and 0.9, respectively, from kinetics analysis. Based on the sensitivity analysis, "NO " the production rate is limited by O radicals. At the same time, maximum "NO" occurs at equivalence ratio one from the CFD result due to the higher residence time caused by the burner geometry. The enhancement of turbulence intensity leads to high residence time, intensifying the flame and resulting in a lower lean blowout limit.

DOI:
https://doi.org/10.22034/jast.2025.475929.1208

1 NOMENCLATURE

d	Tube diameter
$D_{i,m}$	Mass diffusion coefficient
$D_{T,i}$	Thermal diffusion coefficient
$\vec{J_i}$	Diffusion flux of species i
R_i	The net rate of production of species i
S_i	Rate of creation by addition from the dispersed phase, plus any user-defined sources
T	Temperature
t	time
Sc_t	Schmidt number
$\vec{v}$	Velocity
Y_i	Mass fraction of species i
Y_i^*	Fine-scale mass fraction of species i
μ_t	Turbulent viscosity
ξ^*	Length fraction of the fine scales
ρ	Density
τ^*	Reacting time

* Corresponding Author's Email: n_nabatian@sbu.ac.ir

Print ISSN:1735-2134 Online ISSN: 2345-3648

2 INTRODUCTION

The world population growth and global energy consumption rates have increased over the last decades. Fossil fuels are the largest source of energy, but they produce great amounts of emissions that lead to climate change. Alternative fuels can provide comparable power with fewer pollutants and conserve conventional fuel sources. Syngas produced from waste products, coal, and biomass is one of the promising alternative fuels [1].

There are several studies focusing on the influence of fuel composition change on combustion characteristics. Some research works have been focused on the addition of hydrogen to hydrocarbons. The hydrogen addition on flame stability and emission production of an atmospheric kerosene/air-premixed combustion was investigated by Frenillot et al. Results indicated that by increasing hydrogen, the stability domain was enhanced, and at leaner combustion, the flame was still stable, leading to lower CO and NO_x emissions [2]. Hydrogen addition to methane/air lean premixed turbulent flame at high pressures was experimentally studied by Griebel et al. Results showed that at the hydrogen-enriched flame, the high OH radical production led to a higher global reaction rate, which resulted in higher flame speed. The lean blowout limit extension was linearly dependent on the hydrogen content of the fuel [3]. The experimental behavior of the Bunsen flame by premixing hydrogen with natural gas was investigated by Vries et al. The hydrogen addition enhanced a flashback risk. Then, the limits of hydrogen addition should be determined based on the safety maintenance and application purpose [4]. The flame speed, ignition time, combustion noise, adiabatic flame temperature, stability limit, and various emissions of natural gas and hydrogen mixture for the cooktop burner were evaluated by Zhao et al. According to the experiments, the combustion performance of a burner did not change with 15% volumetric hydrogen addition, leading to hydrogen utilization flexibility on existing cookers [5]. Hydrogen addition influence on confined swirl-stabilized methane-air combustion was examined by Kim et al. The hydrogen addition increased the NO_x emission, while this effect was reduced at higher swirl intensity or excess air addition [6]. The influence of hydrogen-rich fuels on turbulent combustors using LES and finite-rate four-step mechanisms was numerically investigated by Zhang et al. Results indicated that high hydrogen content leads to the separation of the wake recirculation zone and the central toroidal recirculation zone. Although high hydrogen concentration shortened the chemical reaction time and reduced the turbulent eddies perturbation, the cellular instability increased the flame intensity fluctuations downstream without the effect of heat release [7]. The flame shape and other combustion characteristics for methane, 40% hydrogen-enriched methane, and four other typical syngas compositions were studied by Papafilippou et al. The syngas flames had lower swirl intensity due to high axial velocities, which weakened the inner recirculation zone. The higher laminar flame speed of the syngas made a shorter flame and increased the curvature of the flame front [8]. The methane/air and hydrogen-enriched methane/air flames of the DLE burner model for non-premixed and partially premixed combustions were experimentally investigated by Pignatelli et al. The pilot flame was sensitive to the flame Reynolds number, and the stability range became narrower with increasing hydrogen ratio due to the flashback tendency, while emissions were reduced [9]. CO_2Pignatelli et al. studied the dilution of syngas combustion at atmospheric pressure and high Reynolds number. Results showed that the flame regime was shifted toward richer conditions by affecting both the chemical and thermal effects CO_2. The NO_x emissions increased while CO pollutants showed an opposite trend with CO_2dilution [10].

The influences of changing turbulence intensity on the combustion characteristics have been conducted in many studies. The numerical investigation of the inlet geometry effect on the non-premixed turbulent syngas was performed by Sotoudeh et al. with 3D simulation of the flame using modified k-omega turbulence and EDC reaction models. The constant of turbulent kinetic energy was set to 0.073 to validate the numerical results with experiments. Results showed that a large inlet nozzle led to the movement of the flame downstream, reducing the combustion efficiency [11]. The effect of swirl intensity on the flame structure, stability, and emissions of the CH_4/O_2 premixed flame was experimentally investigated by Choi et al. Results exhibited that the longitudinal distribution of CO concentration inside the combustor was strongly dependent on the swirl intensity, and its optimal value of 0.8 for this combustor was set for flame stability and emission control [12]. The dynamic response of the H_2/CH_4 syngas flame of a partially premixed combustor induced by velocity

modulation in the fuel feed line was experimentally studied by Joo et al. The flame length and flow momentum were enhanced as the concentration of H2 was increased in the syngas composition [13]. The lean premixed syngas turbulent flame at a wide range of turbulent intensities, initial pressures, and hydrogen volumetric fractions was investigated by Zhao et al. The flame became more wrinkled at higher turbulent intensity, and initial pressure led to a larger flame area and turbulent burning velocity. The flame was wrinkled, with convex structures more frequent than concave ones on the flame front. The vortex scale dominated the wrinkled scale, while the smallest wrinkled scale was influenced by the flame's intrinsic instability. The Syngas flames had a much-wrinkled flame front with a smaller cusps structure in comparison to the methane/air ones. Results showed that turbulent intensity was not the only factor in the flame structure, and the shape of the flame played a significant role [14]. The variation of bluff-body lean premixed flame structures with turbulence was experimentally studied by Chowdhury and Cetegen. The flame front had weak corrugations and a symmetric form with continuous heat release at low turbulence intensity, while flamelet merging and localized extinction occurred along the shear layer, and an asymmetric flame shape formed due to high turbulence intensity. The turbulent flame area at high turbulent intensity and the reduced rate were increased [15].

The composition of syngas is dependent on the production method and feedstock. The wide variation in the syngas composition is a challenge that decelerates the popularization of syngas burners and combustors. The laminar and turbulent burning velocities using different kinetic schemes showed a discrepancy between numerical and experimental results at high temperatures, pressures, and equivalence ratios [16]. Therefore, numerical and experimental research on the composition influence of syngas would be insightful in designing burners and combustion chambers.

In this study, the effects of the syngas composition variation on different combustion characteristics from production/consumption rates of major species, O and OH radicals, and LBO limits, and turbulence influence on the φ_{LBO} in the bluff body burner are investigated.

3 REACTION MECHANISM

To model the chemical kinetics of the Perfectly Stirred Reactor (PSR) and 1D freely propagating premixed flame of syngas mixtures in CHEMKIN software, a simplified kinetic mechanism containing 15 species and 46 elementary reactions has been generated from the GRI3.0 mechanism consisting 53 species and 325 elementary reactions using the Directed Relation Graph with Error Propagation (DRGEP) method.

The validation of the reduced mechanism in terms of the laminar flame speeds of (%5 H_2, %95 CO) composition was conducted by comparing the results of the simplified mechanism with the GRI3.0 mechanism ones, as shown in Fig. 1. The obtained laminar flame speeds deduced from the reduced and the GRI3.0 mechanisms are in good agreement with just 2% difference; however the simplified mechanism result is in good agreement with the experimental data [17]. Then, using the reduced mechanism to simulate combustion instead of the GRI3.0 mechanism decreases CPU time consumption up to 75% with high accuracy.

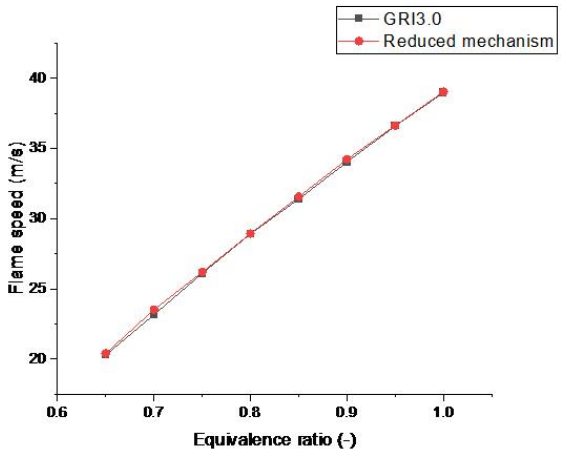

Fig. 1. Flame speeds of (5% H_2, 95% CO) mixture

3. NUMERICAL SIMULATION SET-UP

Figure 2 shows the schematic of the 2D bluff body burner, $d = 0.022m$ which was made in the ANSYS Design Modeler. The mesh convergence test was conducted as shown in Figure 3, and finally, the mesh with 38393 elements and 24753 nodes was selected. From the aerodynamic analysis of the burner, the realizable $k-\varepsilon$ turbulence model for steady cases and the SAS model in unsteady conditions were used to observe the effects of turbulence [18]. The SAS model turbulence model, due to the introduction of the von Karman length scale in its formulation, can precisely predict the unsteady swirling flow formed in the recirculation zone of the flame holder. The

interaction between turbulence and chemistry is evaluated using the ED model. EDC considers small, turbulent structures where reactions occur. The 2-D incompressible Favre-averaged partial differential equations for density, two velocity components, species mass fractions, enthalpy, turbulent kinetic energy, and turbulent dissipation rate are used to solve conservation equations for chemical species. FLUENT introduces the local mass fraction of each species Y_i, and it is calculated through the convection-diffusion equation.

$$\frac{\partial}{\partial t}(\rho Y_i) + \nabla.(\rho \vec{v} Y_i) = -\nabla.\vec{J}_i + R_i + S_i \qquad (1)$$

where S_i is the creation rate from the dispersed phase addition plus any user-defined source term. The source term in the conservation equation for the mean species i, in Eq. (1), is modeled as

$$R_i = \frac{\rho(\xi^*)^2}{\tau^*[1-(\xi^*)^3]}(Y_i^* - Y_i) \qquad (2)$$

where Y_i^* is the fine-scale species mass fraction after reacting over time τ^* [19]. $\vec{J}_i$represent the diffusion flux of species i due to the concentration and temperature gradients.

$$\vec{J_i} = -\left(\rho D_{i,m} + \frac{\mu_t}{Sc_t}\right)\nabla Y_i - D_{T,i}\frac{\nabla T}{T} \qquad (3)$$

where Sc_t is the turbulent Schmidt number, and its default value is 0.7. The equations are solved for N-1 species, where N is the total number of the fluid phase chemical species.

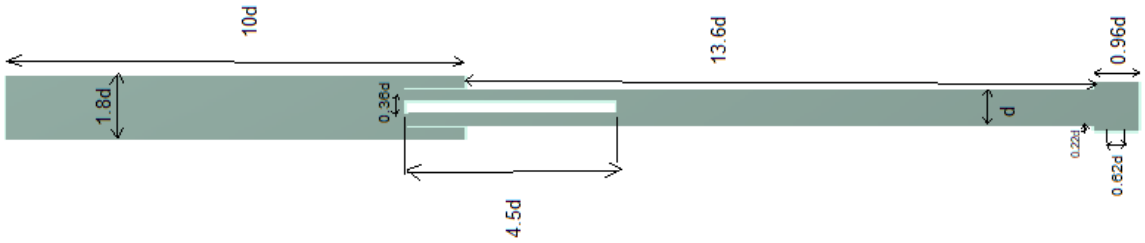

Fig. 2. Schematic of bluff body burner rotated 90 degrees

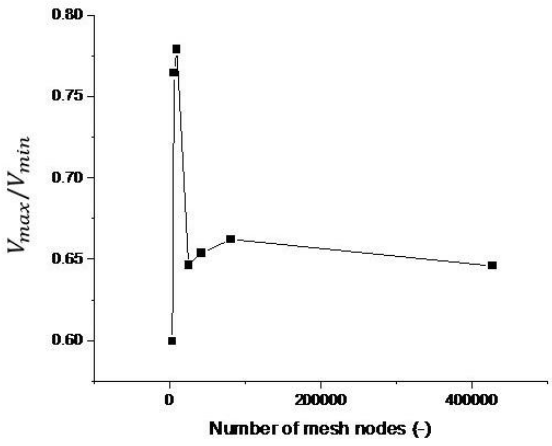

Fig. 3. The ratio of the maximum stream velocity at the outlet to the inlet velocity over the number of mesh nodes

The walls are considered adiabatic with no-slip condition, and the operating pressure is P=1 atm. The inlet velocity is 1 m/s (high residence time) with a turbulence intensity of 1%. To imply different turbulent intensity levels to the flow, a turbulent kinetic energy source is added to the momentum equation in the boundary conditions. Air and syngas mixture are considered well-mixed when entering through the inlet. Figure 4 demonstrates mole fractions of the reactants for the three fuel compositions: (5% H_2 - 95% CO), (25% H_2 - 75% CO), and (50% H_2 - 50% CO) over the equivalence ratios range from 0.3 to 2.

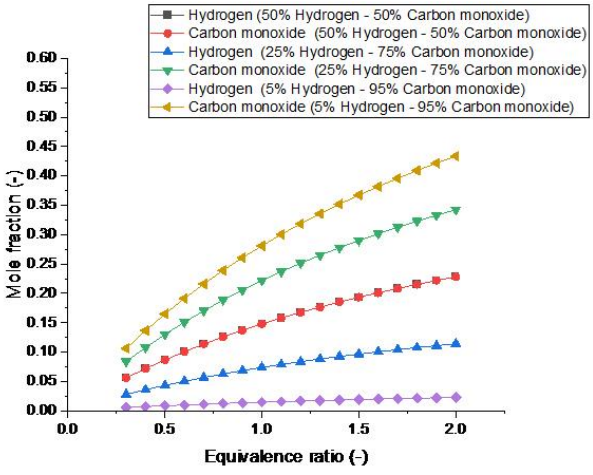

Fig. 4. Mole fraction of the reactants at the inlet of the burner

4 RESULTS AND DISCUSSION

Turbulence and combustion models used in this work have been validated in Ref. [18] for propane flames over the computational domain of Fig. 2, using the experimental results of the previous work [20].

The effects of fuel composition variation on the premixed flame characteristics, including CO and NO_x emissions, dilute flame separation, combustion heat release, flame temperature, and laminar flame speed are studied. At equivalence ratios below 1, as the amount of hydrogen in the fuel composition is increased, the produced CO is decreased, as shown in Fig. 5. The CO is mainly oxidized by OH radicals based on Fig. 6, and by increasing the concentration of hydrogen in the fuel composition, there is no change in the order of the sub-reactions affecting CO consumption; however, the role of the dominant sub-reactions, which consume CO is enhanced.

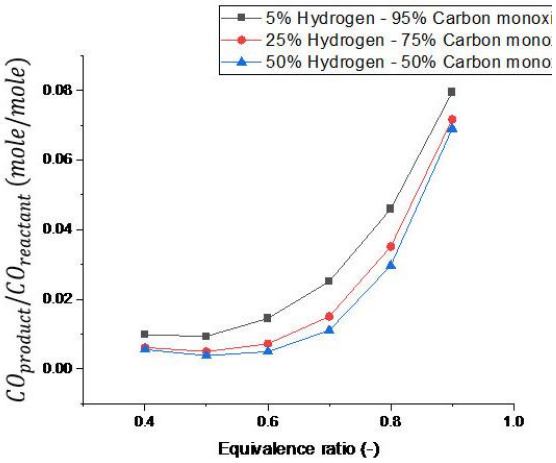

Fig. 5. The ratio of the product CO to the amount of CO in reactants for $\varphi = 0.4 - 0.9$

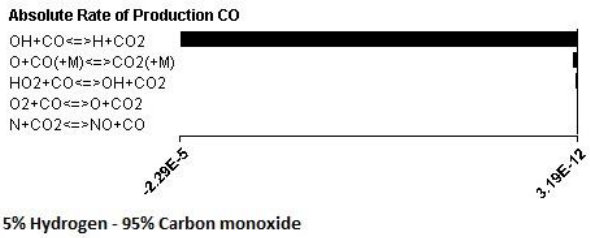

Fig. 6. Dominant sub-reactions affecting CO consumption for three different fuel compositions at $\varphi = 0.4$

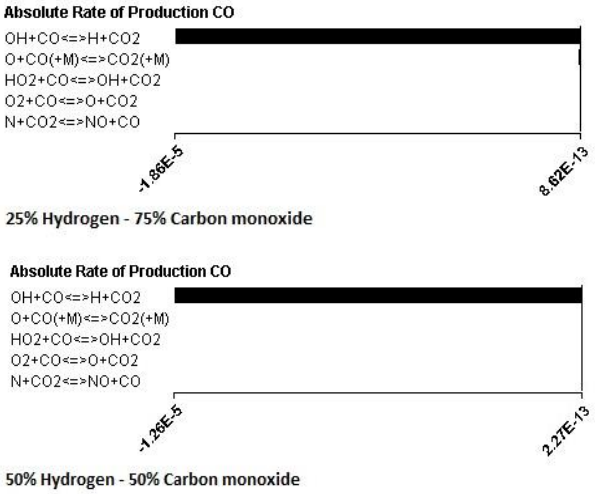

Continue of Fig. 6. Dominant sub-reactions affecting CO consumption for three different fuel compositions at $\varphi = 0.4$

For the fuel composition with 5% hydrogen at lean combustion, the reaction that has the major effect on the amount of OH radicals is the reaction in which OH radicals are consumed by CO as demonstrated in Fig. 7. By increasing the share of hydrogen in the fuel composition to 25 and 50%, the predominant reactions affecting the OH radicals amount are the reactions by which the OH radicals are produced. This indicates that at lean combustion, as the concentration of hydrogen in the fuel composition increases, the production of OH radicals is enhanced, which is confirmed in Fig. 8. As mentioned, the reaction that has the highest impact on CO consumption is the reaction of CO with the OH radicals; thus, increasing hydrogen concentration in the fuel composition leads to lower CO emissions at lean combustion.

Using the kinematic analysis of CHEMKIN, the LBO equivalence ratios for three fuel compositions with 5, 25, and 50% hydrogen are determined in ANSYS FLUENT. Due to the unstable nature of the flame structure, the SAS turbulence model with the EDC model is utilized to study the flame's behavior at the LBO limit, and results are given in Table 1. It shows that with hydrogen concentration enhancement in the fuel composition, the LBO equivalence ratio decreases. Flame separation occurs when the amount of heat generated by combustion is less than the heat required for the initiation of the fuel and air mixture combustion for a laminar flame condition.

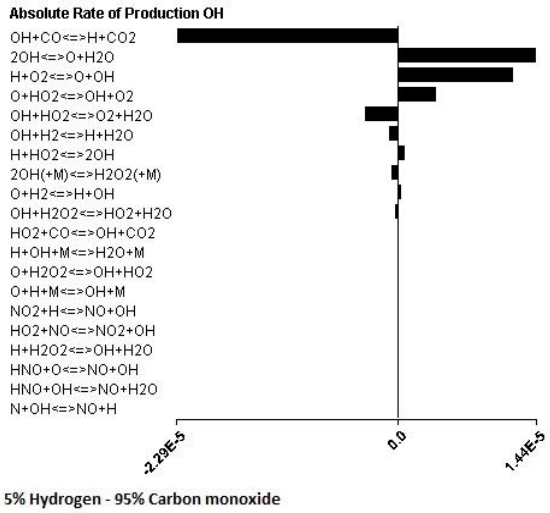

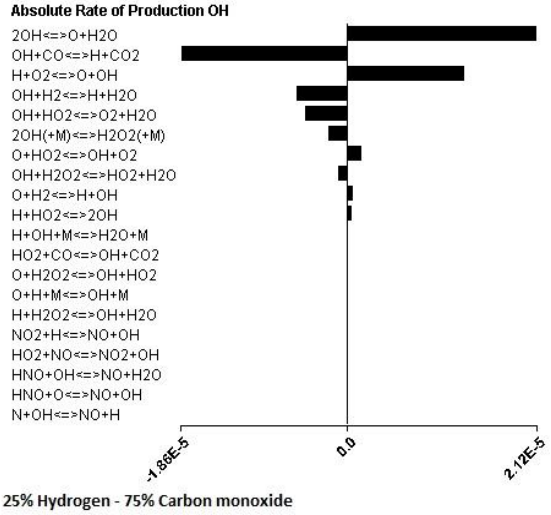

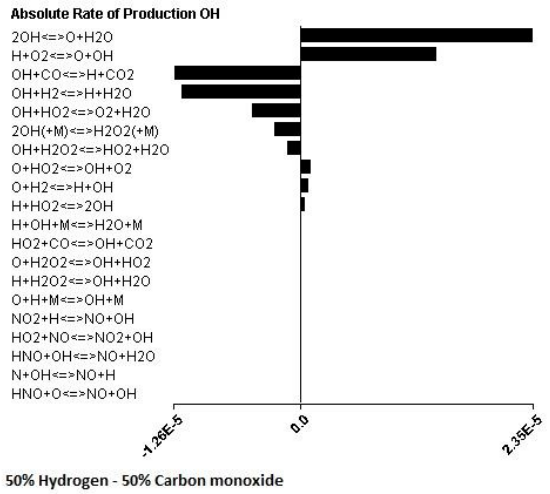

Fig. 7. Sub-reactions affecting the production and consumption of OH radicals at $\varphi = 0.4$.

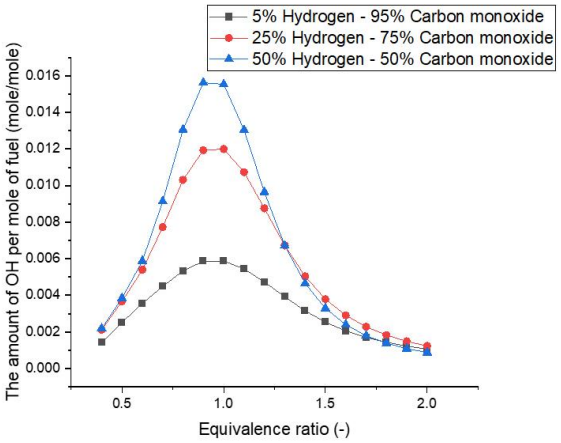

Fig. 8. The amount of OH radicals produced in the combustion of one mole of fuel.

Using the kinematic analysis of CHEMKIN, the LBO equivalence ratios for three fuel compositions with 5, 25, and 50% hydrogen are determined in ANSYS FLUENT. Due to the unstable nature of the flame structure, the SAS turbulence model with the EDC model is utilized to study the flame's behavior at the LBO limit, and results are given in Table 1. It shows that with hydrogen concentration enhancement in the fuel composition, the LBO equivalence ratio decreases. Flame separation occurs when the amount of heat generated by combustion is less than the heat required for the initiation of the fuel and air mixture combustion for a laminar flame condition.

Table 1. LBO equivalence ratio of three fuels with 5, 25, and 50% hydrogen

Fuel composition	φ_{LBO}
5% H_2- 95% CO	0.35
25% H_2- 75% CO	0.32
50% H_2- 50% CO	0.31

Figure 9 shows the combustion heat release per mole of the three fuel compositions. As the volumetric percentage of hydrogen in the fuel composition increases, the heat generated by the combustion of one mole of fuel is slightly reduced. The reason is that the heating value of the hydrogen combustion is slightly lower than the heating value of the CO combustion. The composition of the fuel with more hydrogen requires less activation energy, and increasing hydrogen concentration in the fuel blend enhances the CO consumption rate. However, increasing hydrogen content in the fuel blend reduces the combustion heat release, which has a negative effect on flame stability; CO consumption rate and

flame speed simultaneously enhance, which assists flame stability. Thus, the overall influence of increasing the share of hydrogen in syngas leads to a more stable flame.

As shown in Figures 10 to 12, for the fuel composition with 5, 25, and 50% hydrogen content, by decreasing the equivalence ratio to a certain point where the generated heat from combustion is less than the required combustion activation energy by the fuel and air mixture, part of the flame becomes thinner and separates from the bluff body. Therefore, a partial extinction of the flame occurs at this location, and the flame begins to separate.

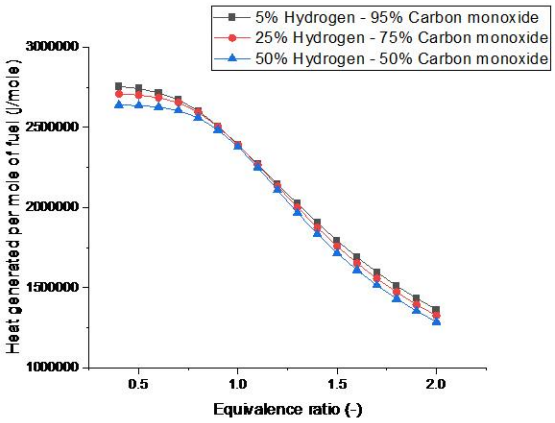

Fig. 9. The heat generated by the combustion of one mole of three fuel compositions with 5, 25, and 50% hydrogen

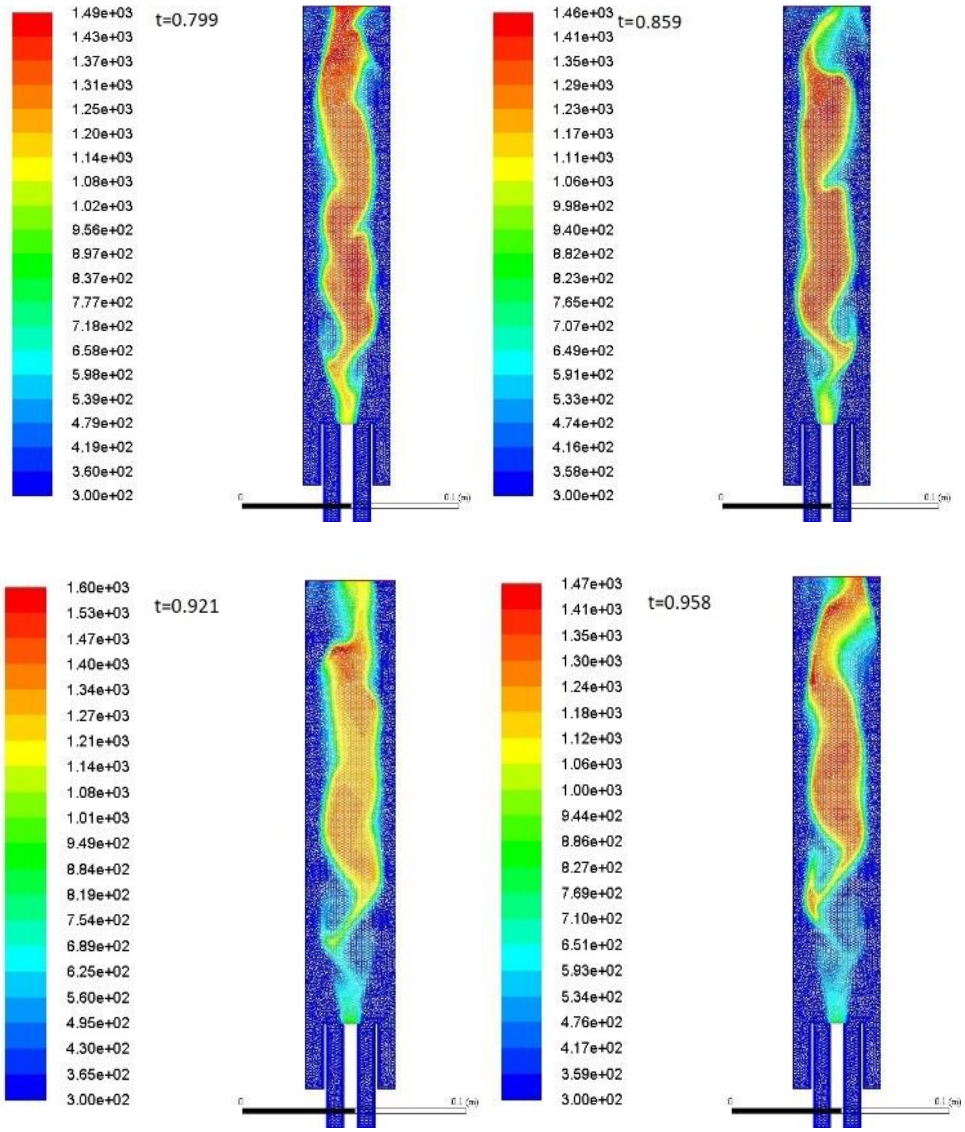

Fig. 10. Flame blowout with 5% H_2

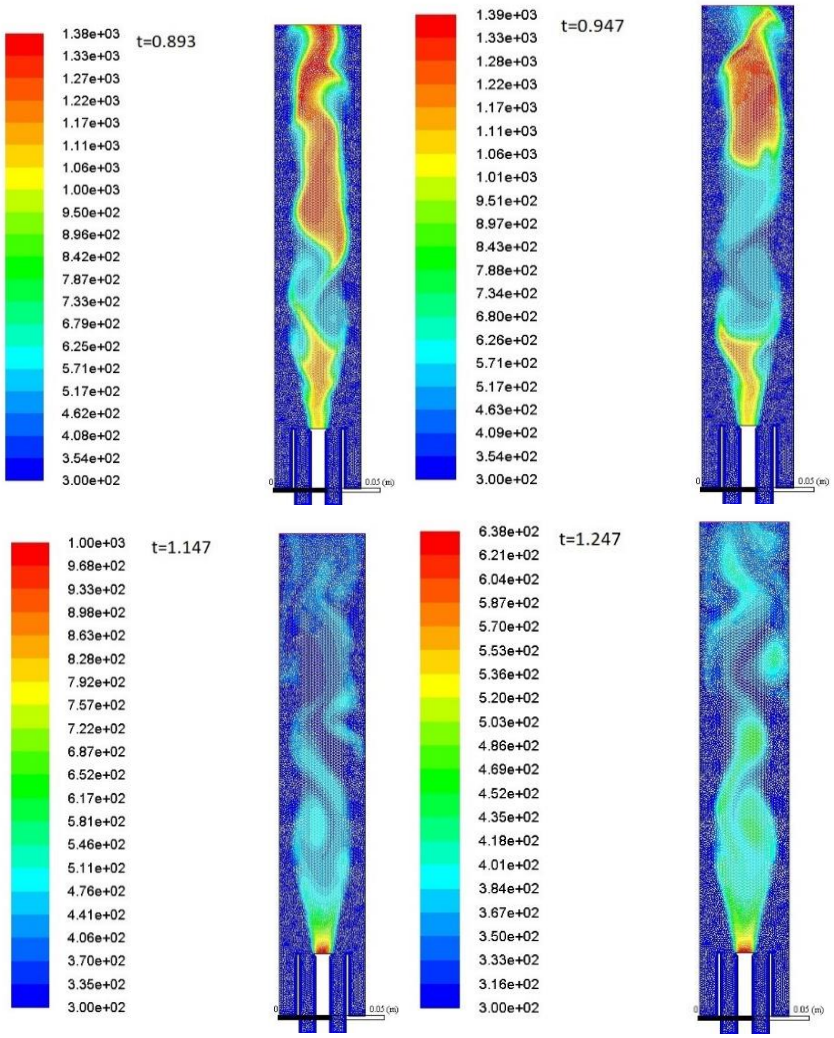

Fig. 11. Flame blowout with 25% H_2

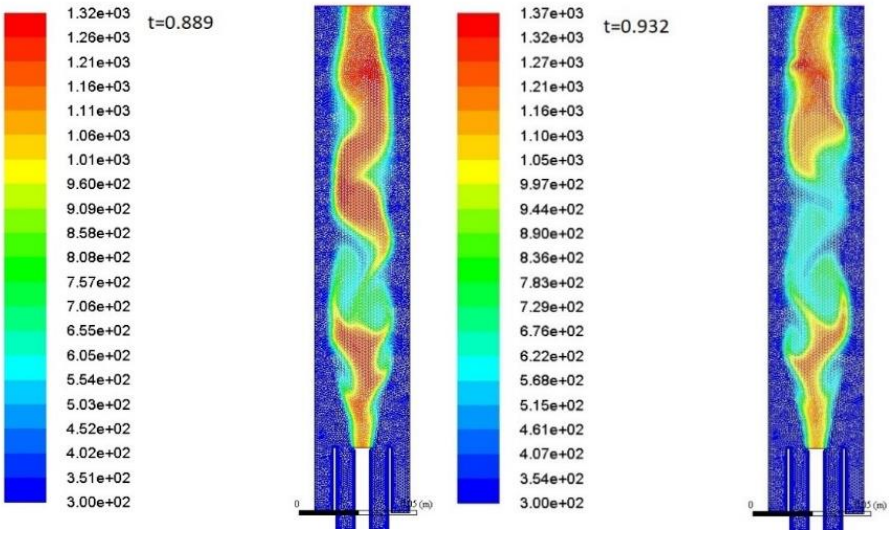

Fig. 12. Flame blowout with 50% H_2

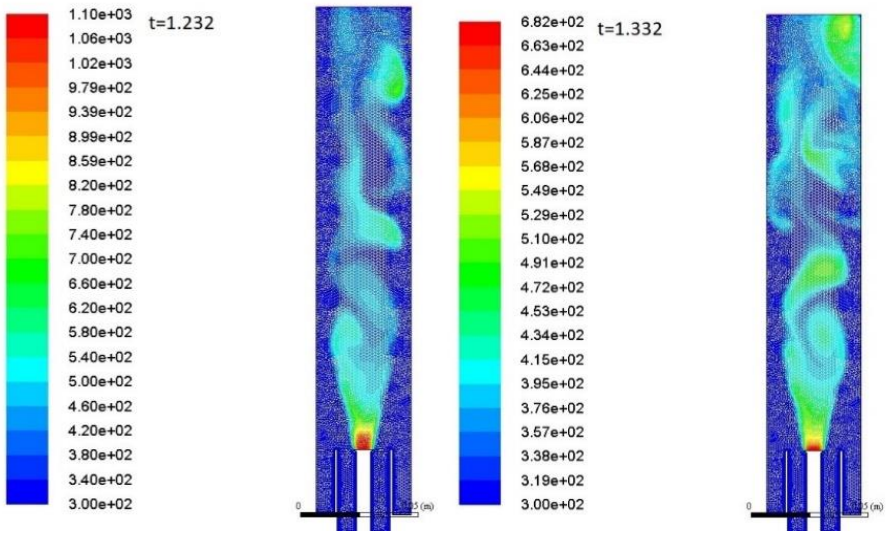

Continue of Fig. 12. Flame blowout with 50% H_2

At the flame separation process of the fuel composition with 5% hydrogen, as shown in Fig. 10, the flame near the bluff body is weak, and the flame completely detaches from the bluff body at once and then exits the combustion chamber. However, in the separation process of the fuel compositions with 25 and 50% hydrogen, laminar flame speeds are higher based on Fig. 13. As a result, the flame near the bluff body is intensified and part of the flame still anchors to the bluff body and extinguishes later by exchanging heat with fresh fuel and air while the other part of it separates at a distance after the recirculation zone as shown in Fig. 14. This indicates that by increasing the concentration of hydrogen in the fuel composition from 5 to 25 and 50 percent, it takes a while for the flame to be completely extinguished. This change can be beneficial in the design of control systems for the burner, by which time can be used to recover the flame on the threshold of extinction.

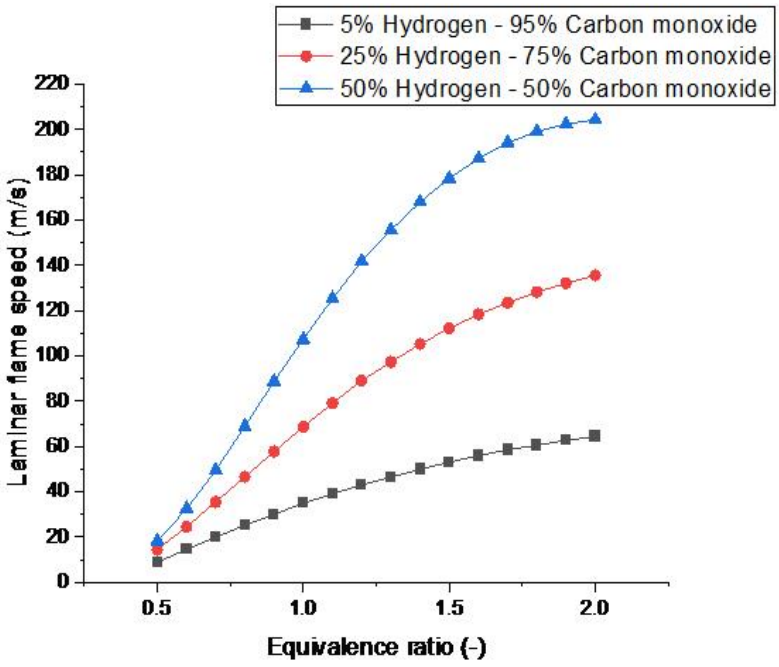

Figure 13. Laminar flame speeds of 3 syngas compositions

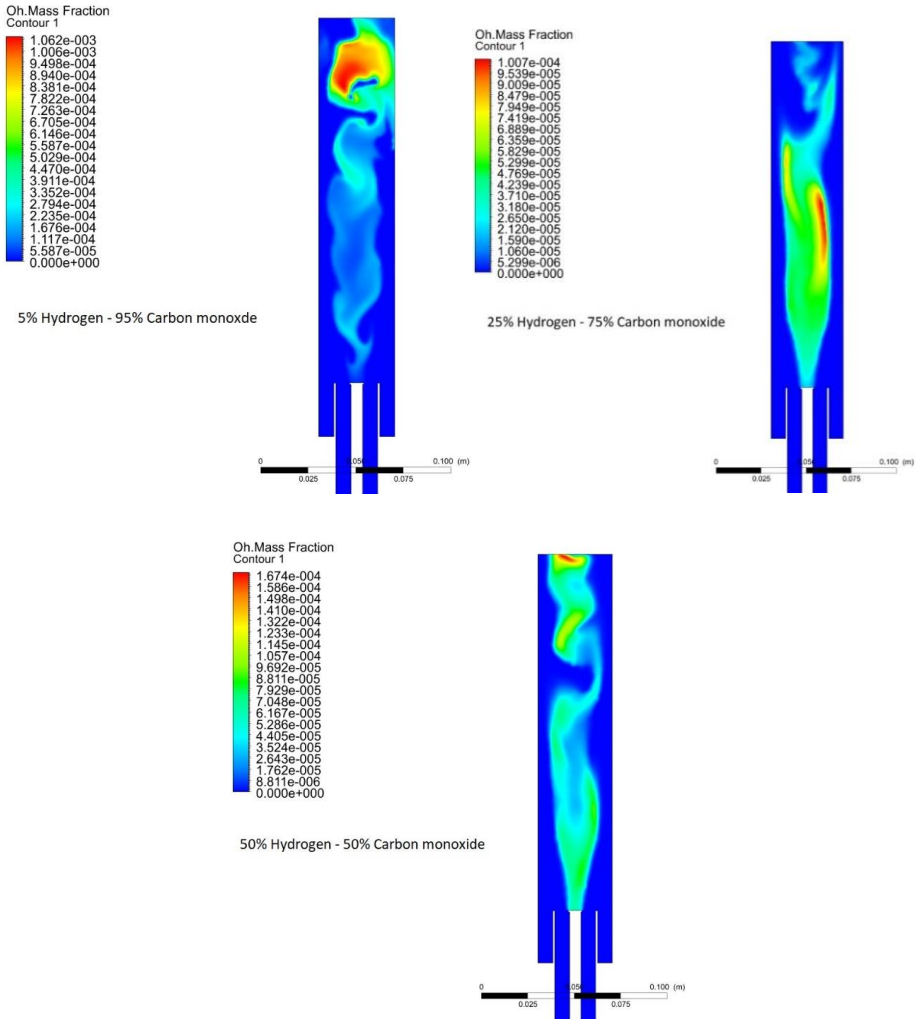

Figure 14. OH radical contours for three fuel composition flames at $\varphi = 0.5$

Figure 15 shows the amount of CO pollutants produced by burning one mole of CO from fuel compositions with 5, 25, and 50 volumetric percent of hydrogen at equivalence ratios of 1 and above.

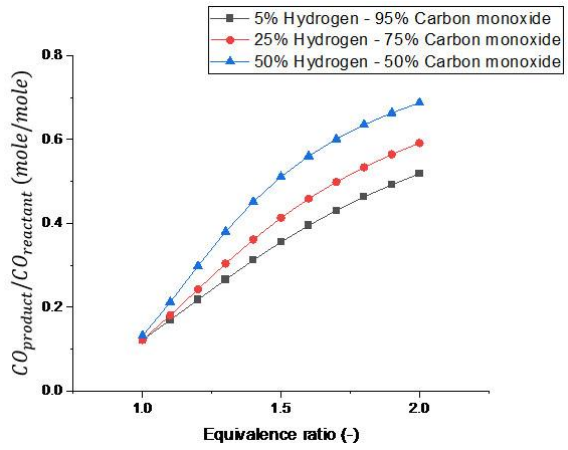

Fig. 15. The ratio of CO in production to the amount of CO in reactants for rich combustion

With hydrogen addition at rich combustion, the amount of CO consumption decreases, and the CO emissions from combustion increase. Figure 16 shows the main sub-reactions on CO consumption in the combustion of syngas with 5, 25, and 50 percent hydrogen at an equivalence ratio of 2.

At the equivalence ratio of 2, as shown in Fig. 16, OH and O radicals have the greatest effects on CO consumption, respectively. Figures 17 and 18 indicate major sub-reactions with the largest effects on the consumption of O and OH radicals, respectively. At$\varphi = 2$, the oxygen amount is less than the amount required for complete combustion. By increasing hydrogen content in the fuel blend, Oradicals are consumed mainly by hydrogen, due to the higher reactivity of hydrogen in comparison toCO. As shown in Fig. 18, for the fuel composition with 5% hydrogen, the OH radicals are mostly consumed in reaction withCO. However, for the fuel composition with 25%

hydrogen, in comparison to the case with 5% hydrogen, the share of OH radicals consumed by hydrogen increases, and similar behavior continues for the fuel mixture with 50% hydrogen. Since the O and OH radicals have the greatest effect on CO consumption, as the amount of hydrogen in the fuel composition increases, fewer O and OH radicals are available to react with CO. Thus, at rich combustion, the more hydrogen added per mole of CO in the fuel leads to the less CO consumption.

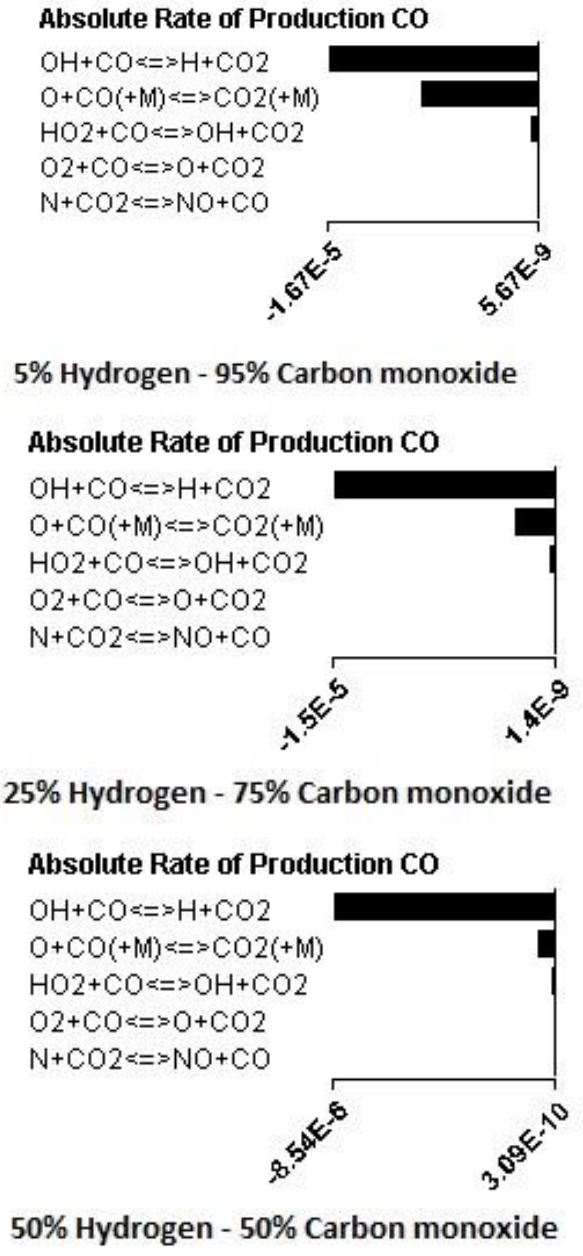

Fig. 16. Major sub-reactions on CO consumption for different fuel compositions at $\varphi = 2$

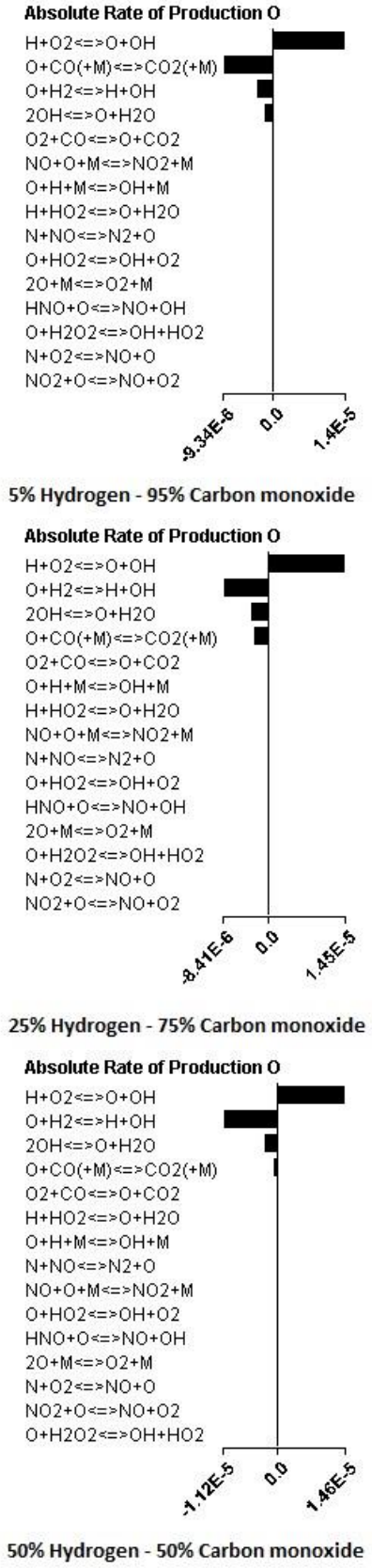

Fig. 17. Major sub-reactions of O radical consumption for different fuel compositions at $\varphi = 2$

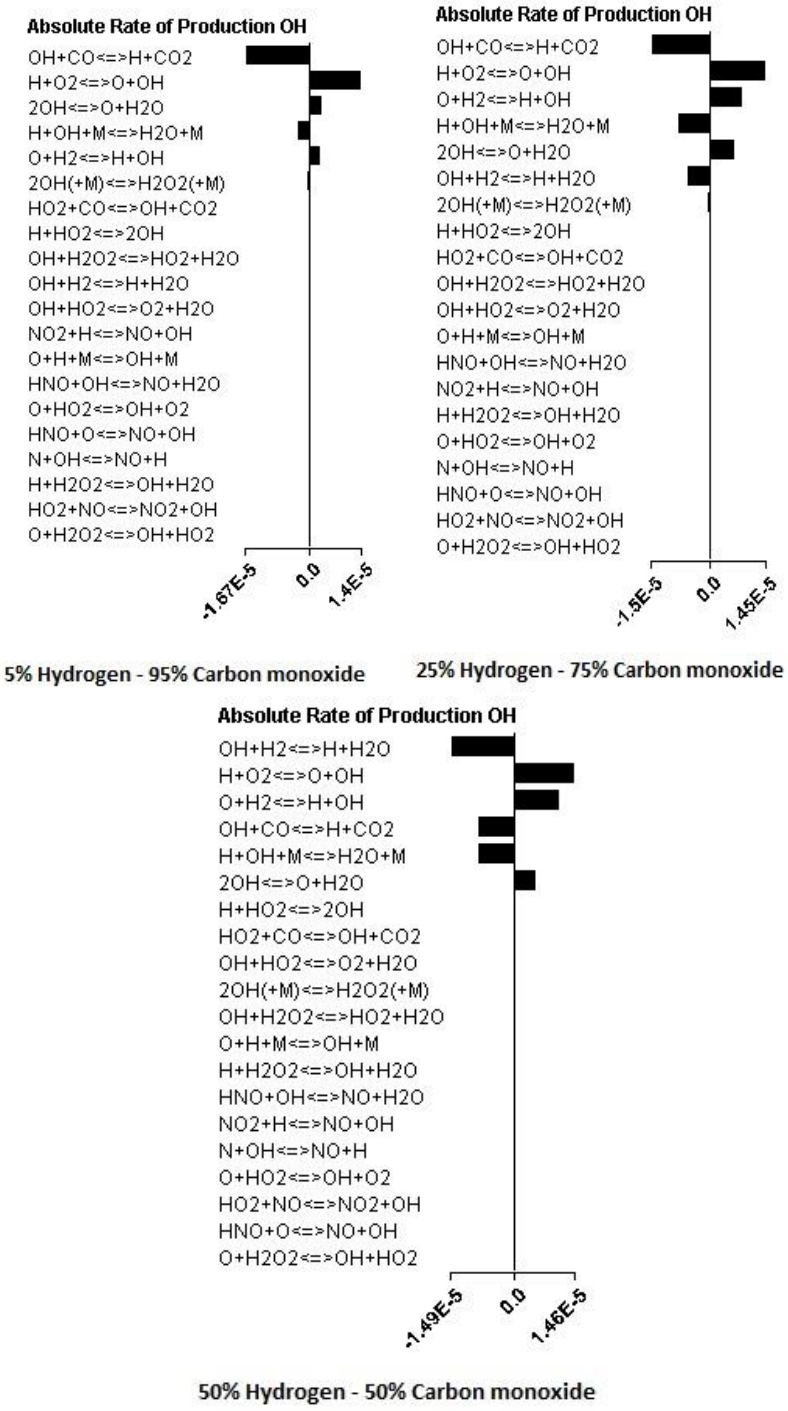

Fig. 18. Major sub-reactions of OH radical consumption for different fuel compositions at $\varphi = 2$

Figure 19 shows the flame temperature of three different fuel compositions. The flame temperature decreases by increasing the share of hydrogen in the fuel composition. According to Figure 9, it was previously shown that by changing the percentage of hydrogen in the fuel composition, the heat generated by the combustion does not significantly change. However, with hydrogen addition to CO, the major combustion products change from CO_2 to the combination of CO_2 and vapor. Since the heat capacity of vapor is higher than the heat capacity of carbon dioxide, the temperature of the flame containing more hydrogen is lower.

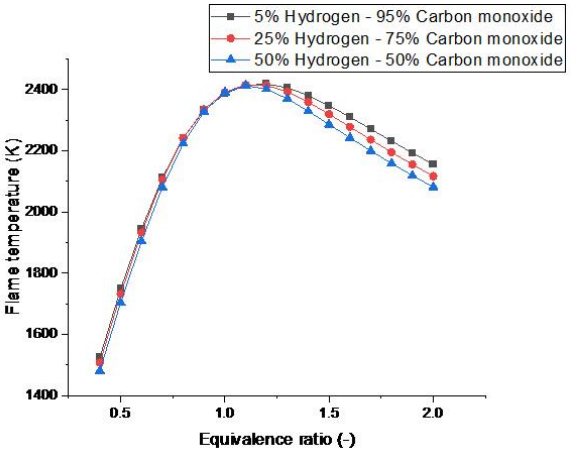

Fig. 19. Flame temperature of three fuel compositions

The number of moles of nitrogen monoxide produced per unit heat of combustion is given in Fig. 20. As the volumetric percentage of hydrogen in the fuel composition increases, nitrogen monoxide production per unit heat of combustion decreases. This can be due to the reduction of maximum flame temperature. Comparison of figures 20 (a) and (b) for three different fuel compositions exhibits the same behavior of NO_x production resulted from CHEMKIN and FLUENT software.

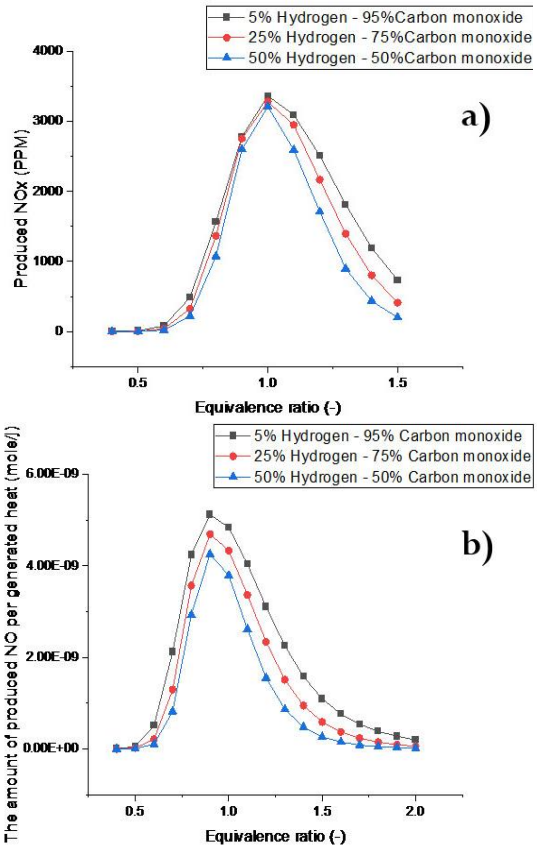

Fig. 20. Produced NO_x emissions of the combustion for three fuel compositions at the outlet of the combustion chamber (CFD simulation) (a) and PSR (chemical kinetics simulation) (b)

The maximum flame temperature for all three syngas variations occurred at $\varphi = 1.1$ (Fig. 19), and the maximum NO production per generated heat is observed at $\varphi = 0.9$ (Fig. 20 (b)). Normalized sensitivity of NO for all three syngas compositions followed the same pattern over the equivalence ratios of 0.9, 1, 1.1; therefore, only the normalized sensitivity of NO for (5% H_2 – 95% CO) is shown in Fig. 21. Based on Fig. 21, production rate of NO depends mostly on the reaction of Nitrogen (N_2) with O radical. Since N_2 is one of the major species in the combustion, O radical is expected to limit the production rate of NO. Figure 22 shows the produced O radical per mole of fuel; by increasing the equivalence ratio from 0.9 to 1.1, O radical is continuously decreased. This explains the maximization of NO at $\varphi = 0.9$. CFD results show that the maximum NO production occurs at $\varphi = 1$ (Fig. 20 (a)); this is due to the difference between the residence time of the chemical kinetics and CFD. Residence time in chemical kinetics simulations was considered constant (0.1 seconds), while in CFD, it depends on the flow characteristics formed by the burner geometry.

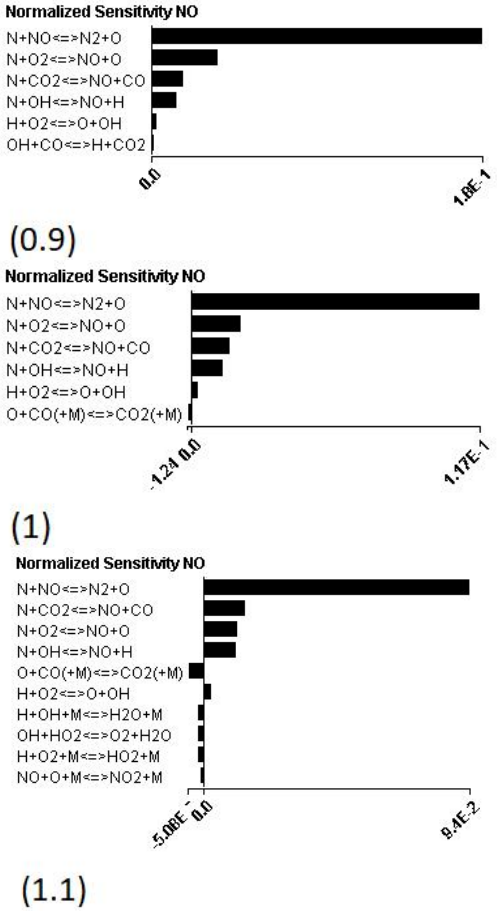

Fig. 21. Normalized sensitivity of NO for (5% hydrogen – 95% CO) flames for $\varphi = 0.9,1,1.1$

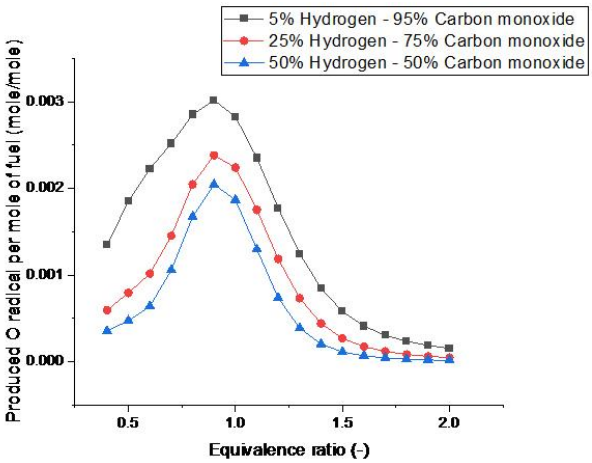

Fig. 22. Produced O radical per mole of the three fuel variations

Finally, different turbulence intensity levels have been applied to flames of three syngas compositions to investigate the LBO limit. Based on the results, increasing turbulence intensities by up to 40% continuously reduces the LBO equivalence ratios, as shown in Table 2.

Table 2. LBO equivalence ratio of syngas compositions for flames with 40% turbulence intensity

Fuel composition	φ_{LBO}
5% H_2- 95% CO	0.31
25% H_2- 75% CO	0.28
50% H_2- 50% CO	0.27

By increasing turbulent intensity, flames of three syngas compositions get stronger near the bluff body (Fig. 23) in comparison to Fig. 14. In low inlet velocity cases where residence time is high, increasing turbulent intensity levels and stream velocity fluctuations improve the mixing of the fresh fuel and air on the sides with combustion products inside the recirculation zone. Therefore, in low stream velocity cases, by increasing turbulent intensity levels, the LBO limit is reduced. It strengthens the flame close to the bluff body and reduces the LBO equivalence ratio.

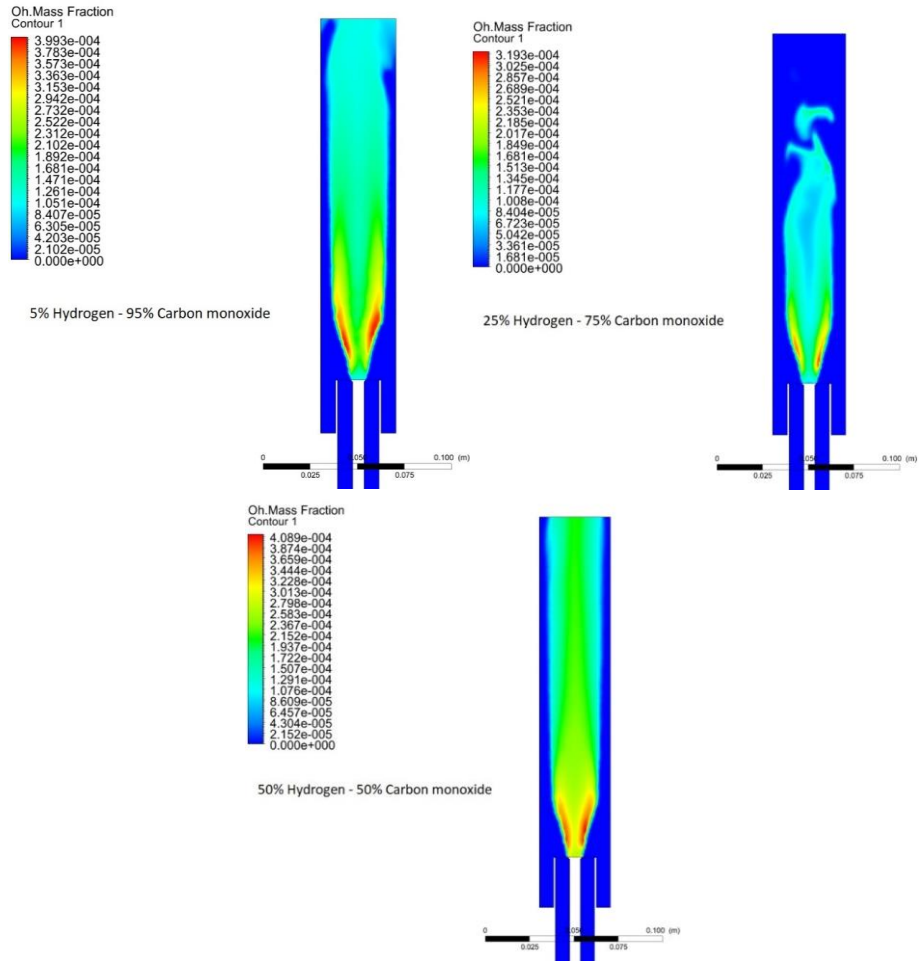

Fig. 23. OH radical contours for three fuel composition flames with 40% turbulence intensity at $\varphi = 0.5$

5 CONCLUSIONS

The simplified mechanism was generated from the GRI 3.0 chemical mechanism using the DRGEP method with high accuracy in comparison to the main mechanism. According to CO and OH radicals consumption rates in dilute combustion, CO radicals are mostly consumed by OH radicals, and increasing the share of hydrogen in syngas increases the amount of OH radicals and, subsequently, CO consumption rate. This explains the increase in flame stability and decrease in LBO equivalence ratios by increasing the hydrogen content of syngas. While in rich combustion, with hydrogen content enhancement in the fuel blend, O and OH radicals tend to react with hydrogen instead of CO, due to hydrogen's higher chemical reactivity compared to CO. Moreover, $O$and OH radicals are the largest consumers ofCO, thus, in rich combustion, by increasing the hydrogen content of the fuel, CO consumption is decreased. Increasing the share of hydrogen in the fuel composition increases the vapor and thermal capacity of the products; consequently, it reduces the flame temperature and produces fewer NO_x emissions. The flame temperature and produced NO were maximized at the equivalence ratios of 1.1 and 0.9, respectively, from chemical kinetics analysis. Sensitivity analysis showed that the production rate of NO is limited by O radicals, which is maximized at the equivalence ratio of 0.9. The peak of NO_x is at $\varphi = 1$ for CFD results due to the difference in the residence time. Although increasing hydrogen content in the fuel blend reduces the combustion heat release, which has a negative effect on flame stability; however, CO consumption rate and flame speed simultaneously enhance, which assists the flame stability. Thus, the overall influence of increasing the share of hydrogen in syngas leads to a more stable flame. By increasing turbulent intensity levels up to 40%, the LBO equivalence ratios in all three syngas composition cases are reduced due to the enhancement in the mixing between fresh fuel and air on the sides of the recirculation zone and combustion products inside of it to burn the remaining unburned reactants. Therefore, in the present bluff-body flame holder with low inlet velocity, increasing turbulence intensity reduces the LBO limit and increases the flame stability.

STATEMENTS & DECLARATIONS

Funding

The authors did not receive support from any organization for the submitted work.

CONFLICTS OF INTEREST

The authors have no relevant financial or non-financial interests to disclose.

REFERENCES

[1] A. M. Briones, S. K. Aggarwal, and V. R. Katta, "Effects of H2 enrichment on the propagation characteristics of CH4-air triple flames," *Combust. Flame*, vol. 153, no. 3, 2008, doi: https://doi.org/10.1016/j.combustflame.2008.02.005.

[2] J. P. Frenillot, G. Cabot, M. Cazalens, B. Renou, and M. A. Boukhalfa, "Impact of H2 addition on flame stability and pollutant emissions for an atmospheric kerosene/air swirled flame of laboratory scaled gas turbine," *Int. J. Hydrogen Energy*, vol. 34, no. 9, 2009, https://doi.org/10.1016/j.ijhydene.2009.02.059.

[3] P. Griebel, E. Boschek, and P. Jansohn, "Lean blowout limits and NOx emissions of turbulent, lean premixed, hydrogen-enriched methane/air flames at high pressure," *J. Eng. Gas Turbines Power*, vol. 129, no. 2, 2007, https://doi.org/10.1115/1.2436568.

[4] H. de Vries, A. V. Mokhov, and H. B. Levinsky, "The impact of natural gas/hydrogen mixtures on the performance of end-use equipment: Interchangeability analysis for domestic appliances," *Appl. Energy*, vol. 208, 2017, https://doi.org/10.1016/j.apenergy.2017.09.049.

[5] Y. Zhao, V. McDonell, and S. Samuelsen, "Influence of hydrogen addition to pipeline natural gas on the combustion performance of a cooktop burner," *Int. J. Hydrogen Energy*, vol. 44, no. 23, 2019, https://doi.org/10.1016/j.ijhydene.2019.03.100.

[6] H. S. Kim, V. K. Arghode, M. B. Linck, and A. K. Gupta, "Hydrogen addition effects in a confined swirl-stabilized methane-air flame," *Int. J. Hydrogen Energy*, vol. 34, no. 2, 2009, https://doi.org/10.1016/j.ijhydene.2008.10.034.

[7] W. Zhang, W. Kong, C. Sui, T. Wang, and L. Peng, "Effect of Hydrogen-Rich Fuels on Turbulent Combustion of Advanced Gas Turbine," *J. Therm. Sci.*, vol. 31, no. 2, 2022, https://doi.org/10.1007/s11630-021-1539-8.

[8] N. Papafilippou, M. A. Chishty, and R. Gebart, "On the Flame Shape in a Premixed Swirl Stabilised Burner and its Dependence on the Laminar Flame Speed," *Flow, Turbul. Combust.*, vol. 108, no. 2, 2022, https://doi.org/10.1007/s10494-021-00279-6.

[9] F. Pignatelli *et al.*, "Pilot impact on turbulent premixed methane/air and hydrogen-enriched methane/air flames in a laboratory-scale gas turbine model combustor," *Int. J. Hydrogen Energy*, vol. 47, no. 60, 2022, https://doi.org/10.1016/j.ijhydene.2022.05.282

[10] F. Pignatelli *et al.*, "Effect of CO2 dilution on structures of premixed syngas/air flames in a gas turbine model combustor," *Combust. Flame*, vol. 255, 2023, https://doi.org/10.1016/j.combustflame.2023.112912

[11] F. Sotoudeh *et al.*, "Geometrical inlet effects on the behavior of a non-premixed fully turbulent syngas combustion; a numerical study," *Acta Astronaut.*, vol. 189, 2021, https://doi.org/10.1016/j.actaastro.2021.08.021

[12] Minsung Choi, Keun Won Choi, Do Won Kang, Hafiz Ali Muhammad, Young Duk Lee, "Experimental investigation of combustion characteristics of a CH4/O2 premixed flame: Effect of swirl intensity on flame structure, flame stability, and emissions," *Case Stud. Therm. Eng.*, vol. 55, 2024, https://doi.org/10.1016/j.csite.2024.104069

[13] S. Joo, S. Kwak, and M. C. Lee, "Effect of fuel line acoustics on the flame dynamics of H2/CH4 syngas in a partially premixed gas turbine combustor," *Fuel*, vol. 285, 2021, https://doi.org/10.1016/j.fuel.2020.119231

[14] H. Zhao, J. Wang, X. Cai, H. Dai, Z. Bian, and Z. Huang, "Flame structure, turbulent burning velocity and its unified scaling for lean syngas/air turbulent expanding flames," *Int. J. Hydrogen Energy*, vol. 46, no. 50, 2021, https://doi.org/10.1016/j.ijhydene.2021.05.090

[15] B. Roy Chowdhury and B. M. Cetegen, "Experimental study of the effects of free-stream turbulence on characteristics and flame structure of bluff-body stabilized conical lean premixed flames," *Combust. Flame*, vol. 178, 2017, https://doi.org/10.1016/j.combustflame.2016.12.019.

[16] E. V. Jithin, G. K. S. Raghuram, T. V. Keshavamurthy, R. K. Velamati, C. Prathap, and R. J. Varghese, "A review on fundamental combustion characteristics of syngas mixtures and feasibility in combustion devices," *Renewable and Sustainable Energy Reviews*, vol. 146, 2021, https://doi.org/10.1016/j.rser.2021.111178

[17] J. Natarajan, T. Lieuwen, and J. Seitzman, "Laminar flame speeds of H2/CO mixtures: Effect of CO2 dilution, preheat temperature, and pressure," *Combust. Flame*, vol. 151, no. 1–2, 2007, https://doi.org/10.1016/j.combustflame.2007.05.003.

[18] N. Nabatian, "Numerical investigation of the premixed V-flame stabilization and blowout," *Mech. Eng. Sharif*, vol. 37, no. 2, pp. 57–67, 2022, (in Persian) https://doi.org/10.24200/j40.2021.57579.1578.

[19] B. MAGNUSSEN, "On the structure of turbulence and a generalized eddy dissipation concept for chemical reaction in turbulent flow," 1981. doi: 10.2514/6.1981-42, https://doi.org/10.2514/6.1981-42.

[20] N. Nabatian and M. Farshchi, "Investigation of Premixed V-shaped Flame Response to Acoustic Oscillations," in *3rd Combustion Conference of Iran*, 2010, (in Persian).

HOW TO CITE THIS ATRICLE

N. Nabatian and V. Nourmohammadi, "Effects of Syngas H2/CO Composition and Turbulent Intensity on the Bluff-Body Premixed Combustion Characteristics," *Journal of Aerospace Science and Technology*, Vol. 18, Issue 2, 2025, pp. 1-16.

DOI: https://doi.org/10.22034/jast.2025.475929.1208

URL: https://jast.ias.ir/article_234619.html